Heliyon 7 (2021) e07904

Contents lists available at ScienceDirect

Heliyon

journal homepage: www.cell.com/heliyon

Review article

Extension of hydrodynamic chromatography to DNA fragment sizing and quantitation

Yanan Wang [a], Yingyan Zhou [a], Dongtang Zhang [a], Xiayan Wang [a,**], Shaorong Liu [b,*]

[a] Center of Excellence for Environmental Safety and Biological Effects, Beijing Key Laboratory for Green Catalysis and Separation, Department of Chemistry and Biology, Beijing University of Technology, Beijing 100124, PR China
[b] Department of Chemistry and Biochemistry, University of Oklahoma, Norman, OK, 73019, USA

ARTICLE INFO

Keywords:
Hydrodynamic chromatography
Open tubular column
DNA fragment Sizing
DNA fragment Quantitation
Free solution separation

ABSTRACT

Hydrodynamic chromatography (HDC) is a technique originally developed for separating particles. We have recently extended it to DNA fragment sizing and quantitation. In this review, we focus on this extension. After we briefly introduce the history of HDC, we present the evolution of open tubular HDC for DNA fragment sizing. We cover both the theoretical aspect and the experimental implementation of this technique. We describe various approaches to execute the separation, discuss its representative applications and provide a future perspective of this technique in the conclusion section of this review.

1. Introduction

Chromatography as a separation technique plays a crucial role in the field of analytical chemistry. According to the state of mobile phase, chromatography is categorized into gas chromatography, liquid chromatography, and supercritical-fluid chromatography. Since a liquid is employed as the mobile phase, hydrodynamic chromatography (HDC) belongs to the category of liquid chromatography. Unlike most other kinds of liquid chromatography, HDC is a separation method relying on the molecular size differences. The first HDC-type separation was carried out by Pedersen who separated a protein mixture on a column packed with 20–35 μm impermeable glass spheres in 1962 [1]. In the late 1960s, DiMarzio and Guttman [2, 3, 4] introduced a technique termed as separation by flow which could be recognized as a form of HDC. In the mid-1960s, Small was asked to develop an efficient technique for characterizing the size of a plastisol resin whose particle diameter was around 1 μm and revealed an interesting hydrodynamic phenomenon of these particles after multiple experiments [5]. Small and co-workers [6] published their first HDC paper in 1974. Columns packed with nonporous solid particles were used to separate various colloidal samples, such as polystyrene latexes, carbon black, and colloidal silica. Colloidal particles in the submicron range were successfully separated and their elution order depended on particle size, column packing method and eluent ionic strength. Based on the experimental results, Small also proposed a separation mechanism and named the technique as "Hydrodynamic Chromatography". HDC has shown the potential for particle sizing, however, the size accuracy and size distribution measurements were often uncertain since the validations needed to use transmission electron microscopy (TEM) [7]. With the implementation of multiple detector system, HDC with triple- and quadruple-detectors [8, 9, 10, 11, 12] has been employed to characterize particles including particle size, shape, and structure. Reviews of this work can be found in literature [13].

Because a DNA molecule carries genetic information utilized in life processes of most organisms and some viruses, analysis of DNA is important for molecular biological research. Conventional methods applied for DNA analysis are slab-gel electrophoresis [14] and pulsed-field gel electrophoresis (PFGE) [15]. However, these methods not only include tedious manual operations such as gel preparation and sample loading, but also have low separation speed [16]. In order to improve the efficiencies, reduce the separation time, enhance the resolution and increase the throughput, capillary gel electrophoresis (CGE) [17] and capillary array electrophoresis (CAE) [18] have been proposed. Polymeric sieving matrices used in the above techniques bring new challenges, as the matrices need to be loaded and replaced after each run. These problems can be avoided if the separation can be performed in free solution. Electrophoretic mobilities of all DNA fragments are similar due to the similar mass-to-charge ratios (m/z), thus DNA fragments cannot be resolved by free-solution electrophoresis [19]. After each DNA fragment

* Corresponding author.
** Corresponding author.
E-mail addresses: xiayanwang@bjut.edu.cn (X. Wang), shaorong.liu@ou.edu (S. Liu).

https://doi.org/10.1016/j.heliyon.2021.e07904
Received 5 January 2021; Received in revised form 12 March 2021; Accepted 27 August 2021

was attached with a monodisperse entity, varying *m/z* values could be created. This approach was theoretically proposed by Noolandi [20] in 1992 and experimentally validated to separate DNA fragment effectively in 1998 [22]. In 1994 [21] it was named end-labeled free-solution electrophoresis. With the development of micro- and nano-fabrication technology, entropic trapping [23, 24] and DNA prism [25, 26] have also been utilized to analyze DNA fragments in free solution. High-performance liquid chromatography (HPLC) has been also applied for DNA analysis in free solution with various modes, such as ion-exchange chromatography [27], ion-pair reversed-phase chromatography [28, 29], size exclusion chromatography [30, 31, 32], slalom chromatography [33, 34] and HDC [35, 36]. These approaches avoid the issues caused by viscous gels mentioned above and provide potential alternatives to gel electrophoresis, while the resolutions cannot compete with that of gel electrophoresis. A previous review [37] summarized these approaches for resolving DNA fragments in free solution.

Recently, HDC with narrow columns shows excellent resolving performance for various biomolecules [38, 39, 40]. When our group started working on narrow capillary chromatography to separate some charged anions, it was found that narrow capillary could resolve DNAs from a few base pairs to hundreds of thousands of base pairs in a single run, and this method was expected to be a promising alternative technique for PFGE. An electrostatic interaction mechanism, the wall-layer electrostatic interaction mechanism, was proposed to explain the theoretical mechanism for separation of short DNA molecules [41, 42]. For large DNA molecules, HDC was found to be the primary mechanism for their separations [37]. Owing to its excellent performance for DNA analysis, HDC has been widely studied in recent years. In this review, we focus on this kind of method based on HDC in free solution for DNA fragment sizing and quantitation. Table 1 provides a summary of literatures on HDC for DNA analysis.

2. Fundamental principle of HDC separation

HDC can be performed in either a packed column or an open capillary. Packed column HDC is usually used to characterize particles and polymers [13]. For biomacromolecules, open capillary HDC is proven to be highly successful with great resolutions. The separation principle of packed column HDC is identical to that of open capillary HDC, as the interstitial space among spherical particles in the packed column can be viewed as a series of open capillaries.

Under laminar flow conditions, parabolic or Poiseuille-like flow profile is generated as a pressure is applied to the open tube or the interstitial space of the packed column (see Figure 1a) according to Hagen-Poiseuille law. The flow streamlines near the walls of the tube (or the packing particles) are the smallest, while those in the middle of the tube (or the interstitial spaces among packing particles) are the largest. Because a large DNA in the sample cannot get as close to the wall of the tube (or the packing particles) as a small DNA can, the large DNA migrates through the tube (or among the packing particles) at a higher

Table 1. Literature summary of HDC for DNA analysis.

Category	Column	Analyte	Apparatus	Comment	Reference
Microcapillary HDC	1-μm i.d., 2.5-μm i.d., 5-μm i.d.	1 kbp plus DNA ladder	BaNC-HDC	DNA fragments with a wide size range were resolved in a single run.	[51]
	5-μm i.d.	Lambda DNA Mono Cut Mix, restriction enzyme digested real-world samples	BaNC-HDC	This work concluded that BaNC-HDC could be an excellent alternative to PFGE by comparing these two methods.	[52]
	2-μm i.d.	1 kbp plus DNA ladder, λ *Hind* III digest DNA	BaNC-HDC	A splitting-based microchip injector was developed to achieve injection volume from pL to fL and size and quantity of DNA fragments were obtained simultaneously.	[49]
	2-μm i.d.	λ *Hind* III digest DNA, 100 bp DNA ladder	SML-FSHS	100% mass detection efficiency of single molecules was achieved.	[53]
	1.6-μm i.d.	ds DNA samples (Lambda DNA, *Hind* III digested Lambda DNA, 1 kbp DNA ladder, and Supercoiled DNA Ladder), ss DNA	SML-FSHS	Analysis of DNA conformation changes and binding interactions were performed.	[62]
	2-μm i.d., 5-μm i.d.	*E. coli* single stranded binding protein (SSB)-DNA samples, DNA condensation samples	SML-FSHS	DNA−biomolecule interactions and DNA conformational changes were studied.	[63]
Nanocapillary HDC	500-nm-i.d.	1 kbp DNA ladder, 100 bp DNA ladder	BaNC-HDC	An electrostatic interaction mechanism was proposed to explain the separation process.	[41]
	500-nm i.d.	dT_5, dT_{10}, dT_{15}, dT_{20}, 1 kbp DNA ladder, 100 bp DNA ladder, real-world genotyping samples from *Arabidopsis* plants	BaNC-HDC	Genotyping fragments were resolved to demonstrate the feasibility for real world sample.	[42]
	750-nm i.d.	ultra low range DNA ladder, 100 bp DNA ladder, 1 kbp plus DNA ladder and λDNA	BaNC-HDC	The transport mechanism of confined DNA in narrow channels was studied and four distinct length regions were observed.	[46]
	750-nm i.d.	1 kb plus DNA ladder	BaNC-HDC	This work studied the effect of temperature on DNA separation using BaNC-HDC.	[56]
	750-nm i.d.	A mixture of 10, 25 bp DNA and 50 bp DNA ladder	BaNC-HDC	This work focused on the elution conditions (eluent concentration, and pressure) on DNA separation using BaNC-HDC.	[57]
HDC on chip-capillary hybrid device	2-μm i.d.	1 kbp plus DNA ladder	BaNC-HDC	DNA fragments with a wide size range were resolved at separation efficiency of more than one million theoretical plates per meter.	[50]
	2-μm i.d.	1 kb plus DNA ladder	BaNC-HDC	This work described how to construct and adjust the confocal LIF for BaNC-HDC.	[58]
	2-μm i.d.	1 kb plus DNA ladder, plasmid DNA from *E. coli*	BaNC-HDC	An EOP and a microchip injector were incorporated with BaNC-HDC in this work.	[59]
	2-μm i.d.	1 kb plus DNA ladder	BaNC-HDC	This work integrated multiplex polymerase chain reaction (PCR), on-line dye intercalation into BaNC-HDC for online DNA analysis.	[61]

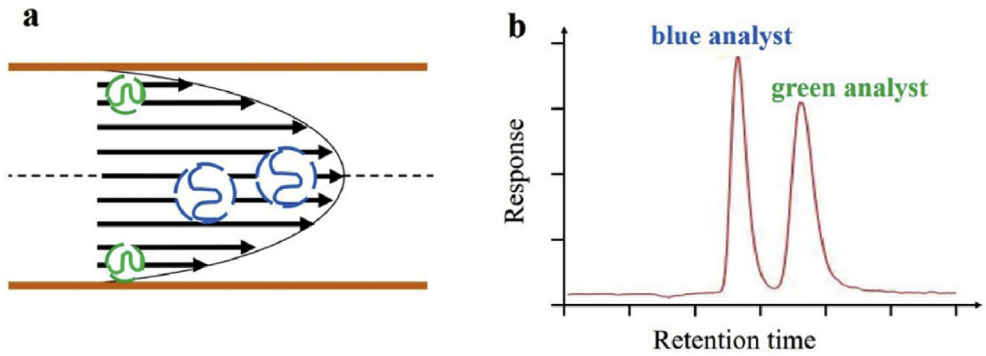

Figure 1. Separation mechanism in HDC. Arrows indicate the flow streamlines. (a) A sample containing two components is injected into an open tubular column and the larger blue analyte resides closer to the center of the column and migrates with a higher average velocity. (b) The larger blue analyte elutes from the column earlier than the smaller green analyte does.

average velocity than a small DNA does. This results in a separation in which a lager DNA elutes earlier than a smaller one does (see Figure 1b) [43].

Various theoretical models have been established to explain the retention mechanism of analytes in HDC. Dimarzio and Guttman [2, 3] introduced a theory which considered hydrodynamic factors only, as well as the theory raised by Brenner and Gaydos [44]. Tijssen et al [45] studied the separation mechanism for polystyrene standards in open microcapillary columns with inner diameters of 1 μm and column volumes of <20 nL. Multiple HDC models based on dilute solutions have been proposed as shown in Table 2, which was assuming that the colloidal forces and tubular pinch effects were absent as well as the interactions with walls. The residence times followed closely with the modified Dimarzio-Guttman and Brenner-Gaydos theories. The macromolecule was considered to be a finite sphere with a diameter of $2a$, and the column diameter was $2R$, the aspect ratio $\lambda = a/R$. A dimensionless residence time, τ, was denoted as the radio of the residence time of the macromolecules to that of the solvent molecules. Linear model I in Table 2 did not consider any the hydrodynamic effects. As for analysis of DNA fragments, the migration behavior in capillary is expressed by quadratic model II, and its derivation is presented in 3.1.

3. Extension of HDC to DNA separation: theory

3.1. Basic mechanism

Figure 2 presents the HDC quadratic model. If we assume a DNA fragment is a solid particle with an equivalent radius of q, its position can be represented by its center. When q is not negligible compared to the bore radius of the separation capillary, the DNA molecule can only reside within the middle region (R-$q \leq r \leq R$) of the capillary. Therefore, a larger DNA fragment spends more time in the center region of the parabolic flow and travels inside the capillary at a higher average velocity which resulted in exiting the column earlier than a smaller one. Wang et al. [46] explained the DNA transport mechanism using HDC quadratic model (model II in Table 2). They assumed that (1) a DNA molecule is small enough to not affect the laminar flow in the capillary, (2) Brownian motion occurs in all possible radial directions of the column cross-section, and (3) the radial diffusion of DNA molecule is fast enough to transport the DNA fragment over the column cross-section many times during the total residence time, *i.e.*, DNA fragments are distributed evenly in the capillary cross-section, then the relative mobility of the DNA molecule, $\overline{\mu_a}$, can be determined by Eq. (1):

Table 2. Theoretical models for residence times in HDC [45].

Model	Aspect radio	Particle type	Equation of calibration curve
I	$\lambda < 0.02$; exclusion only	hard spheres and permeable spheres	$\tau = (1+2\lambda)^{-1}$
II	$\lambda << 1$; exclusion and flow profile	hard spheres and permeable spheres	$\tau = (1+2\lambda-\lambda^2)^{-1}$
III	$\lambda < 1$; exclusion, flow profile, and rotation	hard spheres	$\tau = [1+2\lambda-2.333\lambda^2]^{-1}$
IV	$\lambda < 1$; exclusion, flow profile, and rotation	permeable spheres	$\tau = [1+2\lambda-1.465\lambda^2]^{-1}$
V	$\lambda < 1$; exclusion, flow profile, and rotation	permeable spheres	$\tau = [1+2\lambda-2.698\lambda^2]^{-1}$
VI	$\lambda < 1$; exclusion, flow profile, and rotation	hard spheres	$\tau = [1+2\lambda-4.89\lambda^2]^{-1}$
VII	$\lambda < 1$; exclusion, flow profile, and rotation	permeable spheres	$\tau = [1+2\lambda-4.03\lambda^2]^{-1}$
VIII	$\lambda < 1$; exclusion, flow profile, and rotation	permeable spheres	$\tau = [1+2\lambda-5.26\lambda^2]^{-1}$

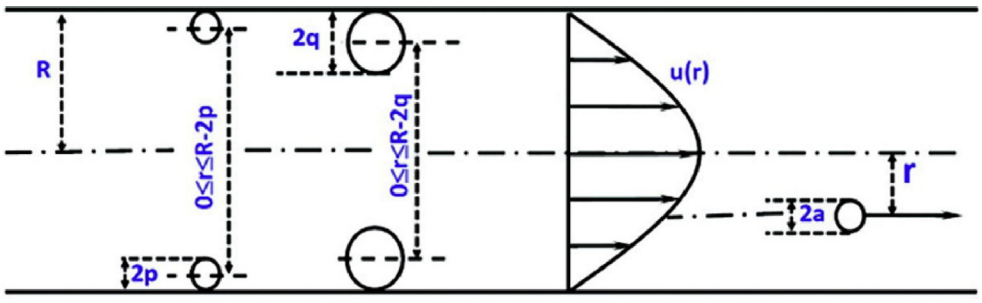

Figure 2. Schematic illustration of HDC quadratic model. (Reprinted with permission from ref. 46. Copyright (2012) American Chemical Society).

$$\overline{u_a} = 2\pi \int_0^{R-a} u(r) \mathrm{n} r dr = \overline{u}(1 + 2\lambda - \lambda^2) \quad (1)$$

or Eq. (2):

$$\overline{\mu_a} = \frac{\overline{u_a}}{\overline{u}} = (1 + 2\lambda - \lambda^2) \quad (2)$$

in which $u(r)$ denotes the velocity profile of a Poiseuille flow, a is the effective radius of DNA molecule, $\lambda = a/R$, $\overline{u}$ represents the average velocity of the eluent.

The residence time of DNA molecule τ can be defined as the radio of the residence time of the DNA molecule to that of the eluent, thus can be calculated as Eq. (3)

$$\tau = \frac{1}{(1 + 2\lambda - \lambda^2)} \quad (3)$$

DNA molecule can be considered as a particle with an effective hydrodynamic radius of R_{HD} [47] which can be estimated by Eq. (4),

$$R_{HD} = c \times L^{\nu} \quad (4)$$

where L represents the DNA size in kbp, ν is the scaling exponent, and c is a constant.

Substituting Eq. (4) into Eq. (2), Eq. (2) then can be written as Eq. (5):

$$\overline{\mu_a} = \frac{\overline{u_a}}{\overline{u}} = 1 + 2 \times \frac{c \times L^{\nu}}{R} - \left(\frac{c \times L^{\nu}}{R}\right)^2 \quad (5)$$

Stein et al. [48] investigated the mobility of DNA molecules driven by pressure in silica channel with height of 175 nm to 3.0 μm using fluorescently labeled DNA by fluorescence microscopy. Three linear DNA fragments with lengths of 48.5 kbp, 20.3 kbp and 8.8 kbp were studied. The corresponding equilibrium DNA coil sizes were 0.73 μm, 0.46 μm and 0.29 μm, respectively. Two distinct behaviors were observed as shown in Figure 3. In channels larger than the DNA coil size, DNA molecules can diffuse freely in the channel. According to the HDC principle described above, long DNA molecules were confined to the center of the channel with the highest fluid velocity, so, increasing the DNA molecular length would increase DNA pressure-driven mobility. In channels smaller than the DNA coil size, the DNA molecules were stretched and squeezed into pancake-like conformation, and the mobility was a constant independent of the channel depth. Furthermore, the difference in lengths of DNA molecules resulted in the difference in widens of the new DNA conformation, while the concentration profiles of DNA molecules across the channel height were length-independent. This explained that same mobilities were obtained for long and short DNA molecules in this region. However, this paper is short of providing a mathematic model to evaluate DNA fragment size based on the measured mobility.

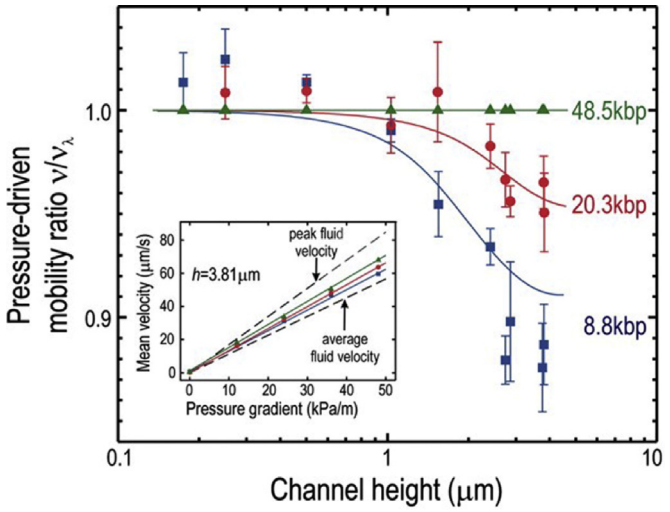

Figure 3. Dependence of DNA mobility on molecule length and channel height. (Reprinted with permission from ref. 48. Copyright (2006) National Academy of Sciences, U.S.A.).

Wang et al. [46] studied the transport mechanism of DNA confined in a 750-nm-radius capillary using double-stranded DNA fragments ranging from 10 bp to 1.9 Mbp under pressure-driven conditions following Eq. (5). Relationship between the relative mobility of the DNA molecule ($\overline{\mu_a}$) and DNA size (L) was obtained as presented in Figure 4. Four distinct size regions were observed in terms of DNA length and termed as rod-like region, free-coiled region, transition region and constant mobility region, respectively. The persistence length of double-stranded DNA was approximately 150 bp. In the rod-like region, DNA molecules shorter than 150 bp behaved like molecular rods. In free-coiled region, the DNA molecules ranging from ~150bp to 2 kbp exhibited the characteristics of freely coiled polymers and their effective hydrodynamic radii R_{HD} were scaled to $L^{0.5}$. Constant mobility region was composed of DNA molecules longer than ~100 kbp which had the same hydrodynamic mobility and could not be resolved. Between the free-coiled region and the constant mobility region, there was a transition region consisted of DNA molecules from ~2 kbp to ~100 kbp. Since the transport mechanism of DNA was complicated in this region, the relative mobility of DNA molecules could not be well fitted with Eq. (5). Surprisingly, if a coefficient kL (where k is a constant) was put into the right-side of Eq. (5), the modified equation worked satisfactorily with good correlation. Furthermore, a 2.5 μm radius capillary was used to observe the transport of DNA molecules. It was found that the four region limits were closely related to the capillary radius, and DNA fragments with different size range could be separated by changing capillary radius.

3.2. Quantitation method

In addition to the size, the quantity is also a basic parameter to characterize DNA molecules. Zhu et al. [49] utilized a narrow open capillary chromatography based on HDC for sizing and quantitation of DNA fragments at zmol to several-molecule level at high-throughput. A flow-splitter-based microchip injector was developed to delivery DNA samples with volumes from pL to fL. A restriction capillary (RC) selector with six different RCs could be enabled to select an appropriate injection volume for analysis as shown in Figure 5a. The narrow capillary column

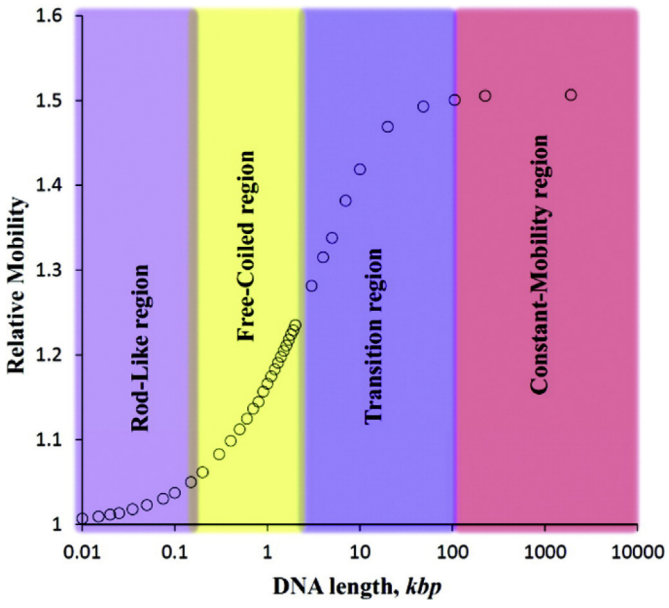

Figure 4. Relationship between DNA relative mobility and its size. (Reprinted with permission from ref. 46. Copyright (2012) American Chemical Society).

(47 cm long, 2 μm i.d., and 200 μm o.d.), the connection capillary (6 cm long, 100 μm i.d., and 375 μm o.d.) and the auxiliary capillary (AC) (15 cm long, 100 μm i.d., and 375 μm o.d.) were connected to a micro fabricated T junction on a microchip (chip-T) at positions 1, 2, and 3, respectively. The other end of the AC was connected to the RC selector. The eluent was divided into two streams by the chip-T, one to a waste reservoir and the other to the narrow capillary. The six restriction capillaries (RC_1-RC_6) had different lengths and same i.d. to achieve an injection volume from 430 fL to 5.7 pL. Relationship between DNA concentration and fluorescence signal (peak area) for 15 DNA fragment standards with different lengths was established for quantitating DNA as shown in Figure 5b. Each linear regression produced excellent linear coefficient ($R^2 > 0.985$). An imperfect feature of this method was that the slope of the calibration curve varies slightly with DNA size. Fortunately, DNA with similar size usually had similar slope. To quantitate a DNA fragment with any size of, for example, b bp, the peak area of the DNA fragment was measured firstly. Then, two calibration curves for two DNA fragments with size of a and c bp where a and c were the closest to b, but $a<b<c$, were located. If the calibration curves were $Y = m_aX$ and $Y = m_cX$ (in which X and Y represented the DNA concentration and the fluorescence signal, respectively) for the two DNA fragments, the sample DNA could be quantified by Eq. (6).

$$Y = \left(\frac{b-a}{c-a}m_c + \frac{c-b}{c-a}m_a\right)X \tag{6}$$

4. Extension of HDC to DNA separation: experimental

4.1. Microcapillary HDC

A HDC approach for DNA fragment analysis using narrow bare open capillary was first developed by Liu's group in 2008 [42], and termed as Bare Narrow Capillary-Hydrodynamic Chromatography (BaNC-HDC) [50]. The experimental setup was presented in Figure 6, and it consisted of a pressure chamber, a bare narrow capillary, and a confocal laser-induced fluorescence (LIF) detector. The sampling end of the capillary was fixed by a septum and dipped into a solution vial inside a pressure chamber. The solution in the vial was driven into the capillary

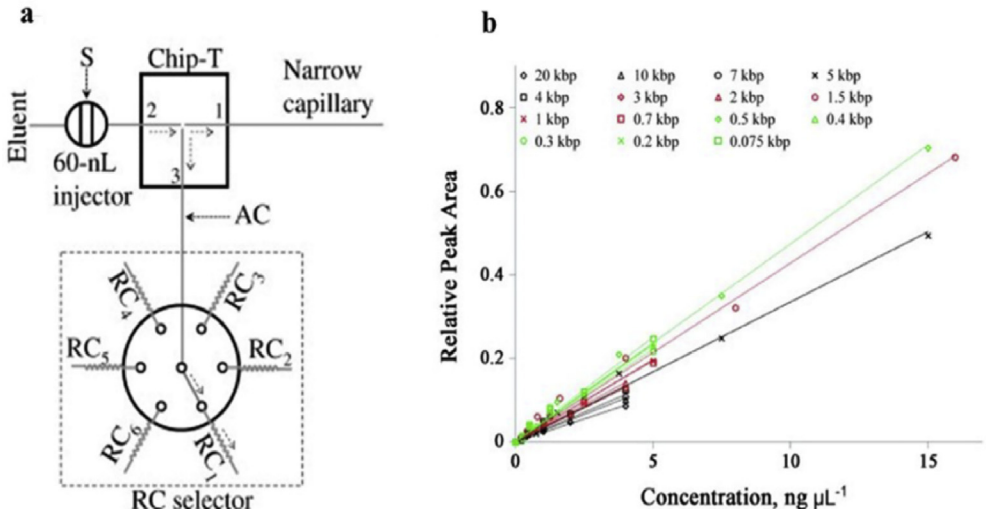

Figure 5. Simultaneously sizing and quantitating DNA fragments at high throughput in HDC. (a) Schematic illustration of the injection scheme for pL-to-fL sample injection. (b) Calibration curves for DNA with different sizes, the linear regression coefficients of the trend-lines were in the range of 0.985–0.991. (Reprinted with permission from ref. 49. Copyright (2014) Wiley-VCH).

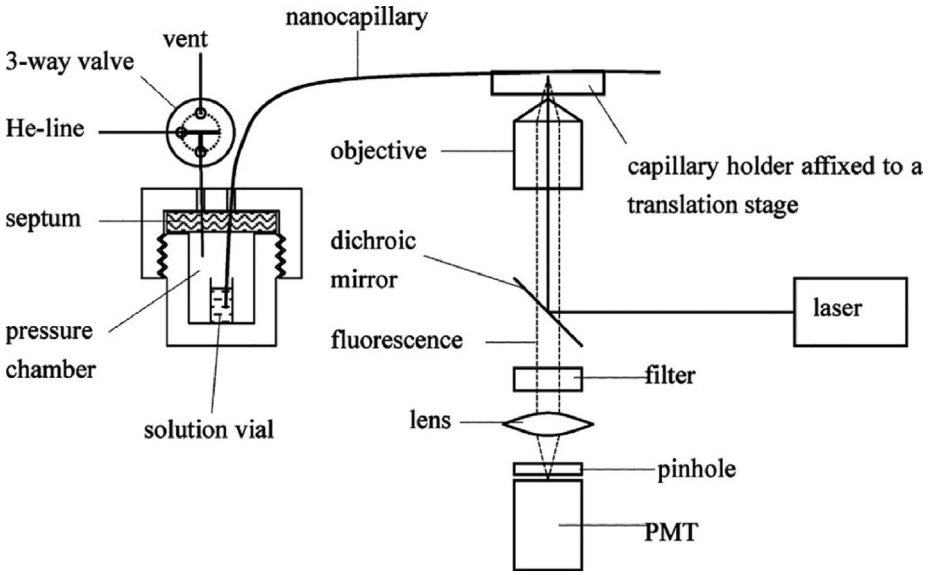

Figure 6. Schematic diagram of BaNC-HDC. (Reprinted with permission from ref. 42. Copyright (2008) American Chemical Society).

by helium gas which was introduced into the pressure chamber and controlled by a pressure regulator. The polyimide coating at an appropriate location on the capillary was removed to form a detection window. The detection window was affixed to a capillary holder that could adjust the window position in three axes to align the window with the optical system. For the LIF detector, a 488 nm beam from an argon ion laser was reflected by a dichroic mirror and focused onto the capillary through an objective lens. The fluorescence of the capillary passed through the dichroic mirror, an interference band-pass filter, a focal lens, and a 1-mm pinhole firstly, and then was collimated by the same objective lens and collected by a photosensor module. The detector output was acquired by a 12-bit D/A convertor and processed by an in-house program written in LabView.

Wang et al. [51] separated DNA fragments with a wide size range in a single run using BaNC-HDC. Capillaries with 1, 2.5 and 5 μm inner radii (r_i) were used, and the separation chromatograms were presented in Figure 7. The 2.5 μm capillary resolved DNA fragments from 75 to 105, 968 bp well, while the 1 μm capillary was good for separating DNA fragments<5 kbp, and the 5 μm capillary was suitable for separating DNA fragments>20 kbp. Generally, large DNA fragments ranging from 10 kbp to 10 Mbp were often separated by PFGE technique [15]. Liu et al. [52] further evaluated the resolution for large DNA fragments with HDC using a 5 μm capillary, PFGE method was also used for comparison. Baseline separation was achieved for DNA fragments ranging from 1.5 kbp to 48.5 kbp with the resolutions less than 9.0 % and the number of theoretical plates were $>10^5$ plates. DNA fragments with small size difference (differed by 6.7 kbp) were well separated using HDC, while they could not be separated by PFGE even after 24 h running on the agarose gel. Sample containing both small and large DNA fragments (0.44 kbp, 7.679 kbp, 18.231 kbp and 119.041kbp) was well-resolved by HDC method, while the DNA fragment of 0.44 kbp was missing in the PFGE profile. Based on these experimental results, they concluded that HDC can be a great alternative to PFGE with improved resolution and separation speed.

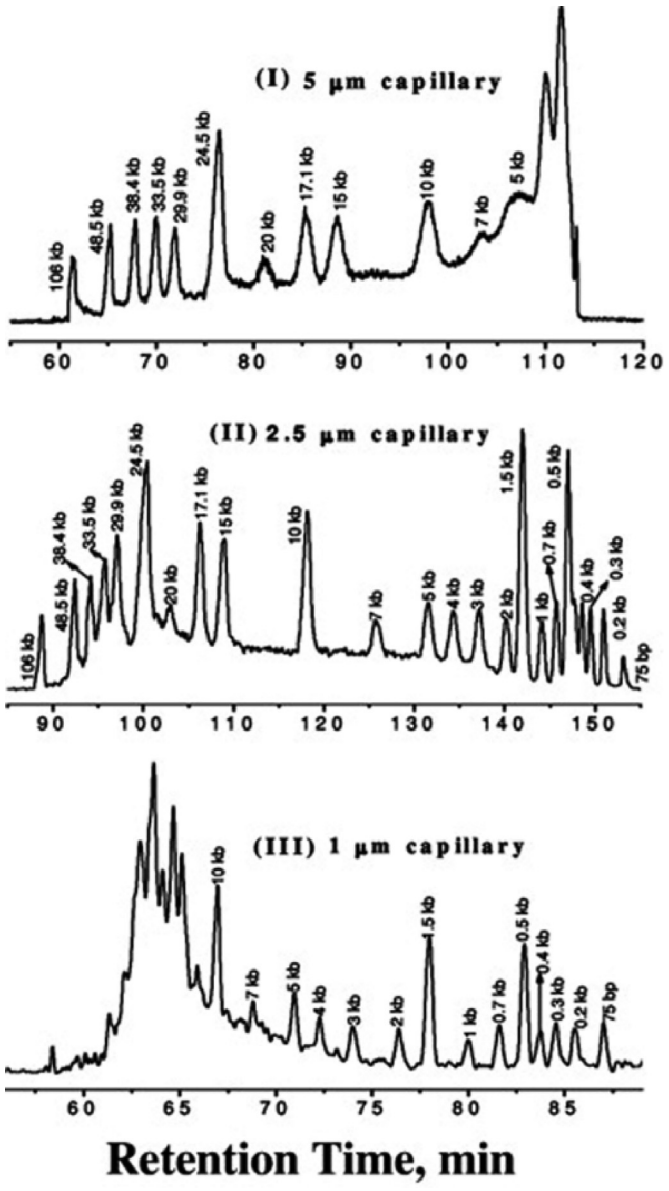

Figure 7. DNA fragments separation results by BaNC-HDC. Conditions: (I) 5 μm r_i and 15 m long (14.95 m effective length) at 350 psi, (II) 2.5 μm r_i and 445 cm long (440 cm effective length) at 360 psi, (III) 1 μm r_i and 75 cm long (70 cm effective length) at 75 psi. 10 mM Tris-1 mM EDTA (pH = 8.0). (Reprinted with permission from ref. 51. Copyright (2010) American Chemical Society).

Liu et al. [53] performed single-molecule analysis of DNA fragment size using single-molecule free solution hydrodynamic separation (SML-FSHS) system illustrated in Figure 8, which integrated a modified confocal spectroscopy system, cylindrical illumination confocal spectroscopy (CICS). into microcapillary HDC. CICS included a cylindrical lens to produce a one-dimensional (1-D) observation volume which can increase mass detection efficiency and a rectangular confocal aperture to minimize noise and maintain single molecule fluorescence burst uniformity [54, 55]. 100% mass detection efficiency of single molecules within the separation capillary was achieved and DNA fragments with wide size range were successfully separated with only 5 pl of sample and 240 ymol (~150 molecules) of DNA.

4.2. Nanocapillary HDC

Nanocapillary chromatography was initially used to resolve some low charged anions and found to show the ability to resolve large DNA fragments occasionally. Wang et al. [42] first realized the DNA fragment separation using a 500-nm-radius capillary under pressure-driven conditions in free solution. The larger DNA fragments were eluted out from the capillary earlier than the smaller ones, which indicated that the elution order of DNA fragments was closely related to their sizes. Four fluorescent dye (FAM)-labeled deoxythymidine (dT) oligonucleotides (dT_5, dT_{10}, dT_{15}, and dT_{20}, in which the subscripts denote the base number in the oligonucleotides) were successfully baseline-separated. And DNA fragments with size range from 500 bp to 10 kbp were separated with higher resolution in 500-nm-radius capillary than in 800-nm-radius capillary, while the DNA fragments were not resolved in a

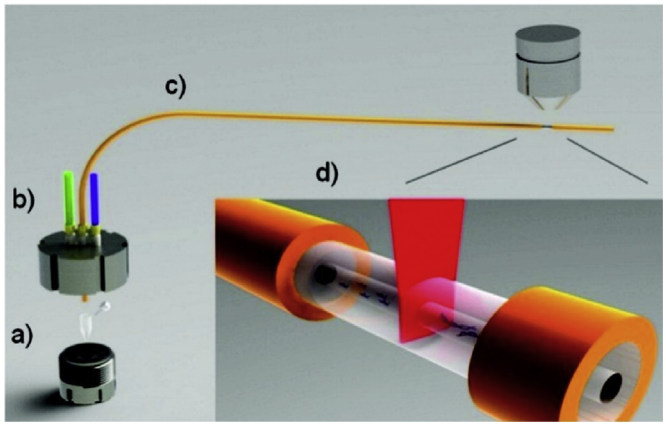

Figure 8. Schematic diagram of the SML-FSHS system. (a) a stainless steel injection chamber, (b) pressure control ports, (c) separation capillary, and (d) CICS analysis region. (Reprinted with permission from ref. 53. Copyright (2010) American Chemical Society).

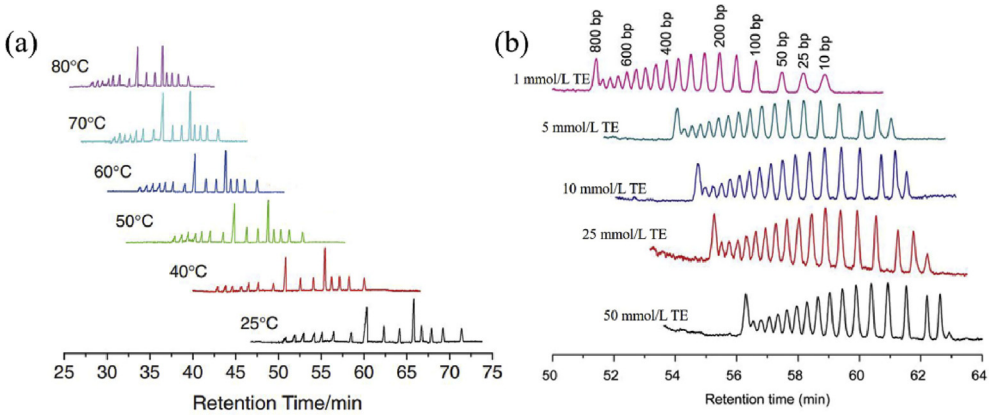

Figure 9. Influence of chromatographic conditions on DNA separation under a 750-nm-radius capillary. (a) Separation results of a 1-kb plus DNA ladder at different temperatures. The separations were carried out in a 70 cm (66 cm effective) long capillary under 200 psi. The sample was injected at 200 psi for 10 s. Peaks from left to right are: 20, 10, 7, 5, 4, 3, 2, 1.5, and 1kb and 700, 500, 400, 300, 200, and 75 bp. (Reprinted with permission from ref. 56. Copyright (2012) The Chemical Society of Japan) (b) Separation results of a mixture of 10 bp DNA fragment, 25 bp DNA fragment and a 50 bp DNA ladder. The separations were carried out in a 144 cm (135 cm effective) long capillary under 1000 psi. The sample was injected at 120 psi for 20 s. Peaks from left to right are: 800, 750, 700, 650, 600, 550, 500, 450, 400, 350, 300, 250, 200, 150, 100, 50, 25, and 10 bp. (Reprinted with permission from ref. 57. Copyright (2015) Springer Nature).

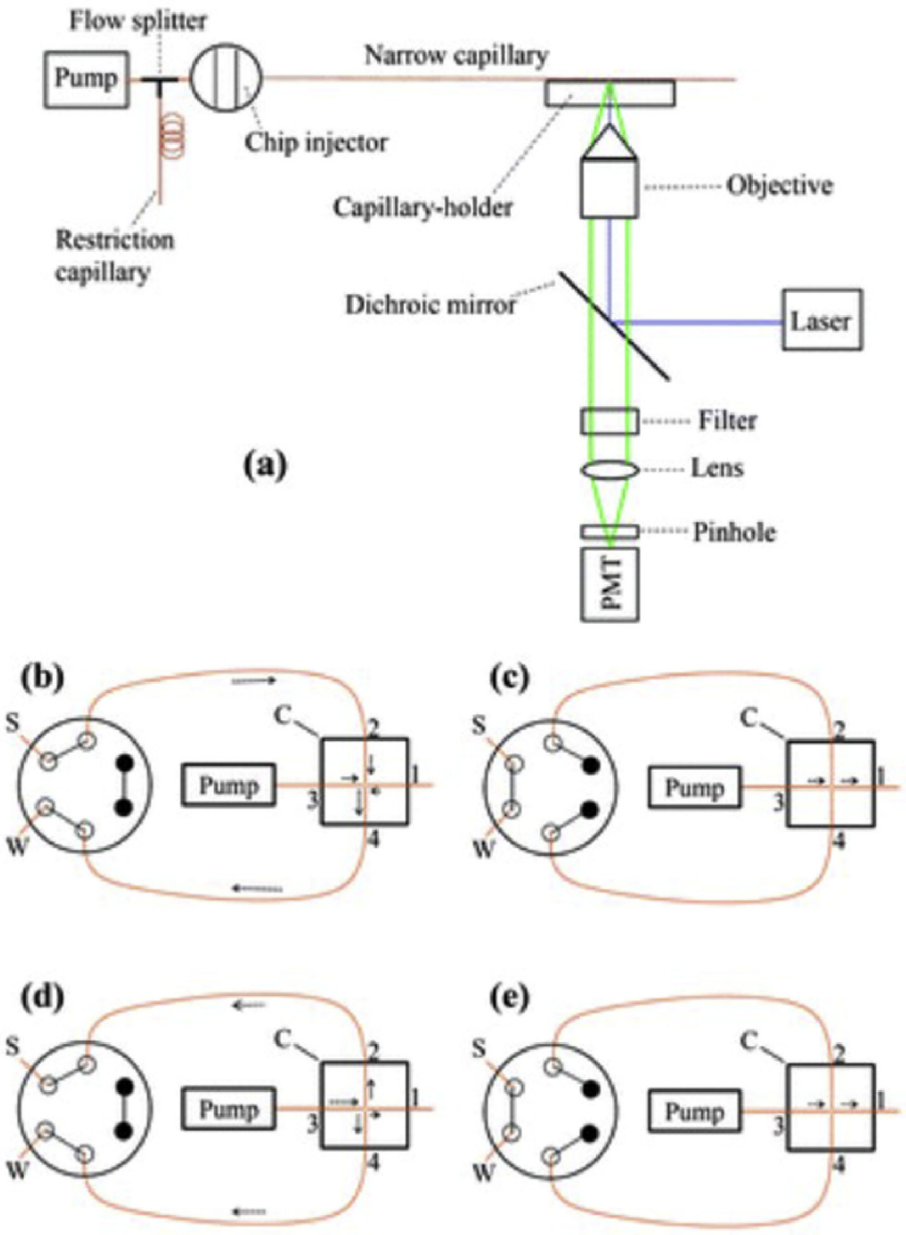

Figure 10. Schematic diagram of the modified BaNC-HDC. (a) Experimental setup. (b)–(e) Schematic diagram depicting the steps of a BaNC–HDC separation: S-Sample, W-Waste, and C-Chip injector. A six-port injection valve is shown on the left. The solid dots represent that these ports are closed. Capillaries connected to positions 1, 2, 3, and 4 on the chip injector are separation capillary, sample capillary, pump capillary, and waste capillary, respectively. The arrows indicate the flow directions. (Reprinted from Ref. [50] with permission from The Royal Society of Chemistry).

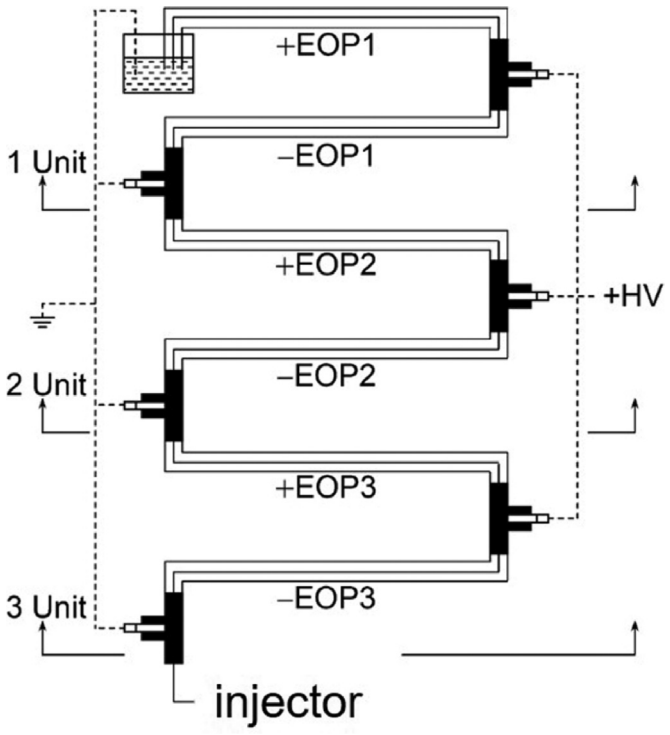

Figure 11. Schematic diagram of EOP for BaNC-HDC. (Adapted with permission from ref. 60. Copyright (2011) American Chemical Society).

3-μm-radius capillary. DNA fragments ranges from 75 bp to 20 kbp were separated with excellent resolution using 500-nm-radius nanocapillary chromatography, and efficiencies of more than 100,000 plates per meter were obtained for many peaks [41].

Chromatographic conditions in DNA separation under a 750-nm-radius capillary including temperature and elution conditions (eluent concentration and elution pressure) have also been studied by Li et al [56] and Liu et al [57], respectively. As the solution viscosity increased with the decreasing temperature, the solution flowed slower at lower temperature, resulting in an increased DNA retention time (see Figure 9a). Increasing eluent concentration also increased retention time (see Figure 9b) as the eluent viscosity increased with its concentration. These increased retention times had induced additional diffusion band broadening. This band broadening effect could be alleviated by enhancing the elution pressure. The authors also noticed that peak shape changed with DNA size and attributed this change to DNA configuration variation; DNA configuration varied with counterion concentrations in eluent.

4.3. HDC on chip-capillary hybrid device

In order to improve the throughput of DNA analysis, a microchip injector was applied by Zhu et al. [50] The modified BaNC-HDC system consisted of a HPLC pump, a flow splitter, a microchip injector, a bare open narrow capillary and a LIF detector as shown in Figure 10a. A six-port valve was utilized to perform the sample injection and carry out the separation. The operation procedure was illustrated in Figure 10b-e. When the two auxiliary capillaries at position 2 and 4 on the chip injector were connected to sample (S) and waste (W), the six-port valve was open (Figure 10b, d); while the six-port valve was closed when the two auxiliary capillaries were connected to the blocked ports (Figure 10c, e). DNA fragments ranging from 75 bp to 20 kbp were well resolved at efficiencies of more than a million plates per meter. Due to the small diameter of the separation column, the on-column LIF detector for BaNC-HDC is not commercially available. Weaver et al [58] describe the details of the construction method of a confocal LIF detector as well as how to adjust and use it for BaNC-HDC. The LIF detector was constructed using a vertical support which was firmly attached to a baseplate. An optical tube containing the objective lens, the dichroic mirror, filter and reflector was bolted onto the vertical support together with a laser holder and a photomultiplier holder. In addition, the X-Z translation stage bolted onto the back of the optical tube was used to align the detection window in the capillary with the objective lens. A solution of 1 μmol/L fluorescein in 10 mmol/L TE buffer was injected to the capillary at a constant flow rate. The alignment was achieved when the output signal of fluorescein reached maximum.

The flow rates for BaNC-HDC by a HPLC pump were generally around a few hundred pL/min, so, a flow splitter with high splitting ratios was

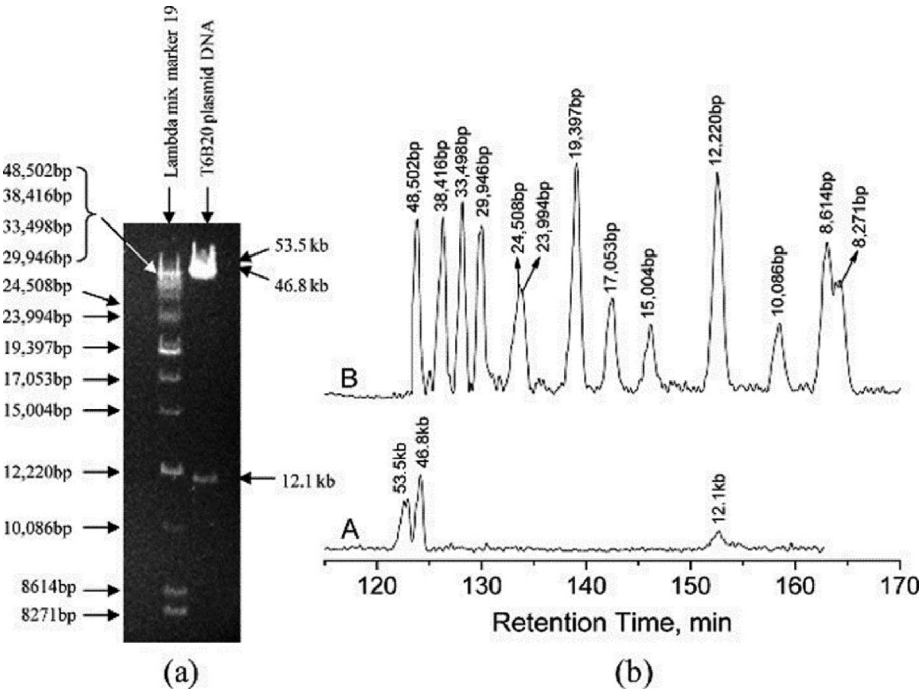

Figure 12. Separation results of *Sac* II digested *Arabidospois* BAC DNA. (a) Agarose gel separation result. (b) BaNC-HDC separation result. The BaNC-HDC separation were carried out in a capillary with a length of 500 cm and an inner diameter of 5 μmunder 350 psi. The eluent contained 10 mM TE. The sample was injected at 80 psi for 8 s. Trace A shows the results from *Sac* II digested *Arabidospois* BAC DNA, and trace B presents the results of 70 ng/μL Lamda Mix Marker 19. (Reprinted with permission from ref. 52. Copyright (2014) American Chemical Society).

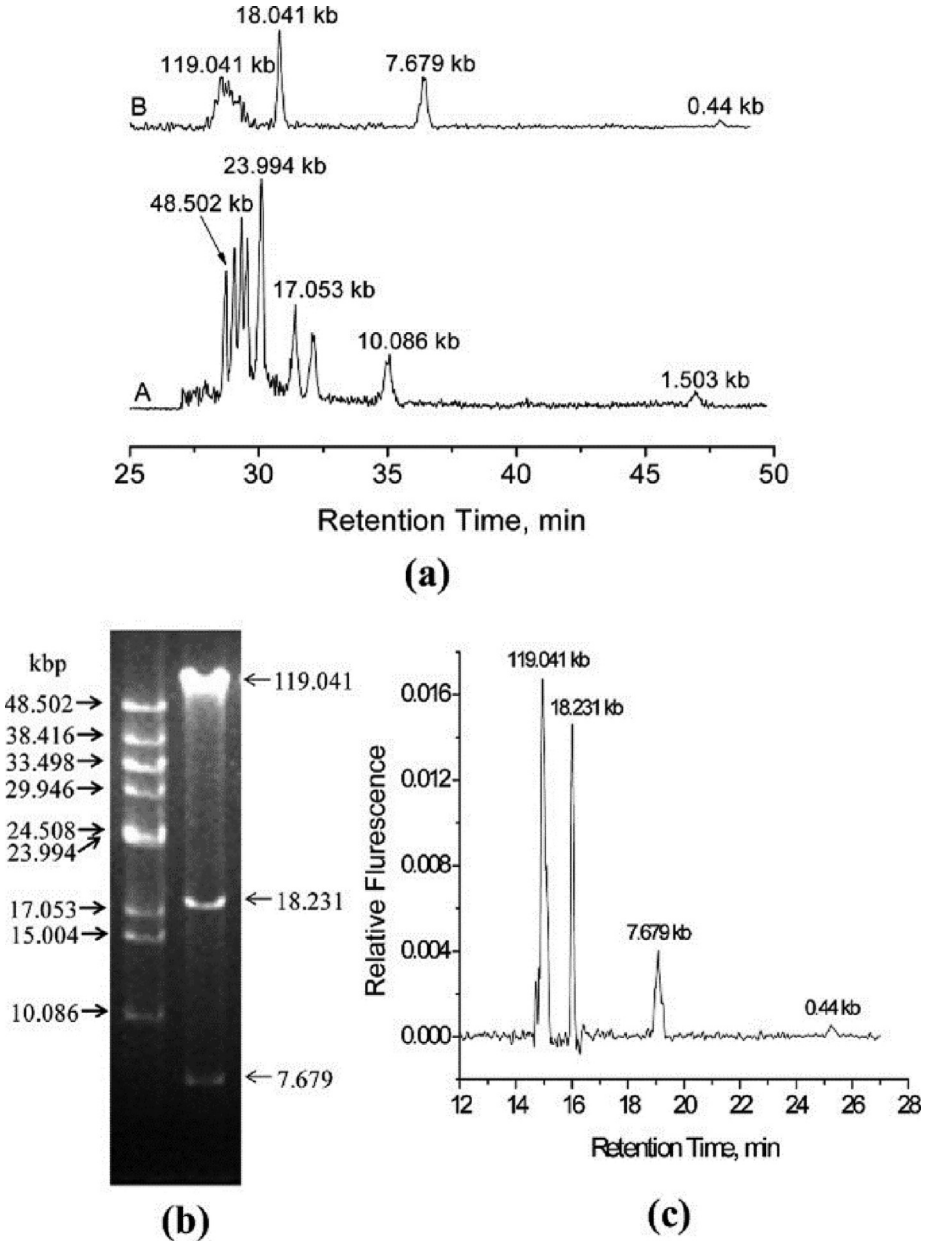

Figure 13. Separation results of PmeI digested Rice BAC DNA. (a) BaNC-HDC separation results. The separation was performed in a capillary with a length of 400 cm and an inner diameter of 5 μm at 40 °C under 900 psi. The eluent contained 10 mM TE. The sample was injected at 100 psi for 15 s. Trace A shows the results of 60 ng/μL LamdaDNA Mono Cut Mix and trace B presents the results from 50 ng/μL PmeI digested Rice BAC DNA. (b) PFGE separation results. (c) Separation results of 50 ng/μL PmeI digested Rice BAC DNA. The separation was performed in a capillary with a length of 250 cm long and an inner diameter of 5 μm at 40 °C under 900 psi. The eluent contained 10 mM TE. The sample was injected at 100 psi for 8 s. (Reprinted with permission from ref. 52. Copyright (2014) American Chemical Society).

needed to use. Zhu et al. [59] replaced the HPLC pump with a high-pressure electroosmotic pump (EOP), which could generate flow rates of several hundred pL/min or even lower. Three basic pump units were stacked in series to increase the pressure output of EOP as shown in Figure 11, each unit was composed of one + EOP and one -EOP. 35 positively coated capillaries were used to construct + EOP, while 35 bare capillaries with negative charged were used to construct -EOP [60]. The 35 capillaries were glued by epoxy adhesive. With the microchip-injector and EOP integrated into BaNC-HDC, the injection could be operated conveniently, the injection volumes could be controlled precisely at picoliter level, and DNA fragments with a wide size range could be resolved at single-molecule level.

Chen et al. [61] integrated multiplex polymerase chain reaction (PCR), on-line dye intercalation into BaNC-HDC for online DNA analysis. The PCR products were labeled by online interaction with YOYO-1 and then separated by BaNC-HDC. To online intercalate with YOYO-1, YOYO-1 was used to flush the bare narrow capillary and adsorb onto the capillary wall firstly, and then DNA molecules were injected to the capillary, meanwhile they would react with the YOYO-1 stored on the capillary wall and online intercalate with the dye. There was no need to recharge YOYO-1 at each separation, and the column can be used for more than 40 runs after the BaNC-HDC column was charged once.

5. Applications

5.1. Real-world sample analysis

To demonstrate the feasibility of this technique in biological application, some real-world samples were also investigated in a few papers.

Liu et al. [52] separated *Sac* II digested *Arabidospois* BAC DNA and PmeI digested Rice BAC DNA by BaNC-HDC. DNA fragments of 53.5, 46.8, and 12.1 kbp sizes were expected to be produced by the *Sac* II digested *Arabidospois* BAC DNA sample. All the expected DNA fragments were clearly separated using BaNC-HDC, while the two large DNA fragments of 53.5 kbp and 46.8 kbp were still not resolved on the agarose gel for running 24 h, shown in Figure 12. Digestion of Rice BAC DNA with restriction enzyme PmeI was expected to generate DNA fragments ranging from 0.44 kbp to 119.041 kbp. All the DNA fragments were baseline-separated by BaNC-HDC in less than 50 min, and the separation time could be decreased to less than 26 min by reducing the capillary

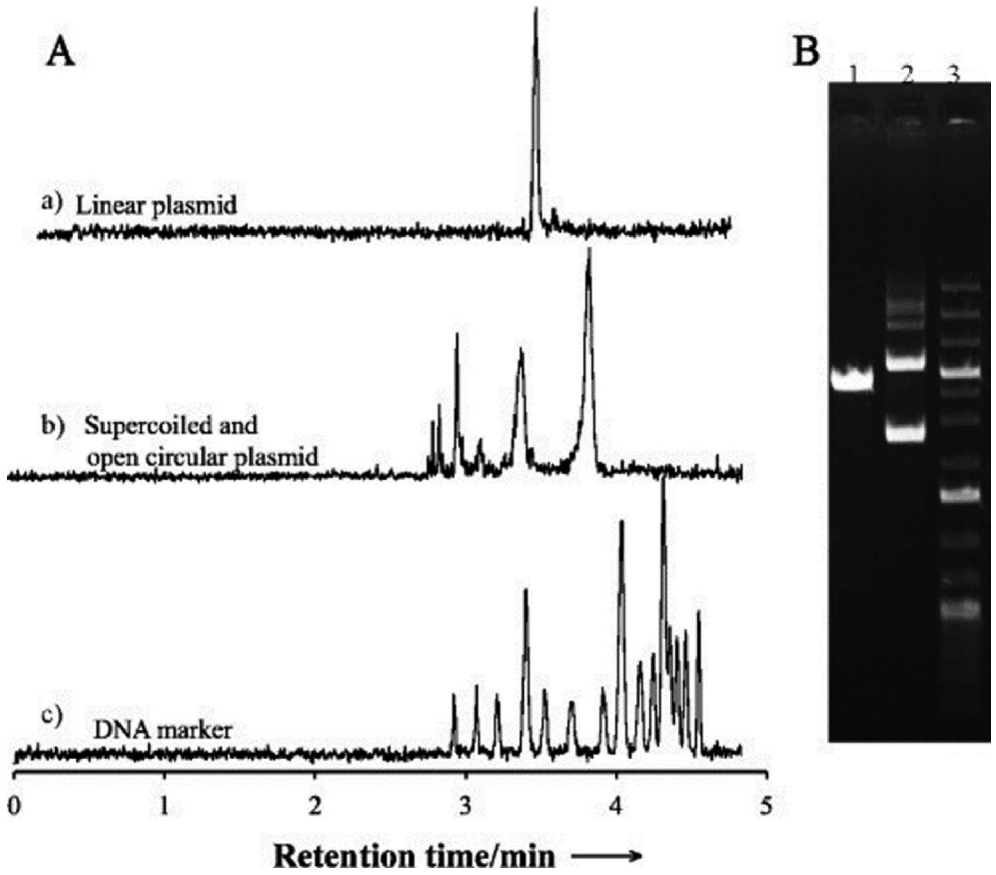

Figure 14. Sizing results of plasmid DNA. (A) BaNC-HDC separation result. The effective length of separation capillary was 65 cm. 5 mm NH_4Ac/NH_4OH (pH 8.0) was used as the eluent. 2.4 pL of sample was injected and the elution pressure was 13.8 MPa. (B) Agarose gel electrophoresis result for the samples. Lane1, 2 and 3 corresponded to Trace a, b, c, respectively. (Reprinted with permission from ref. 59. Copyright (2013) Wiley-VCH).

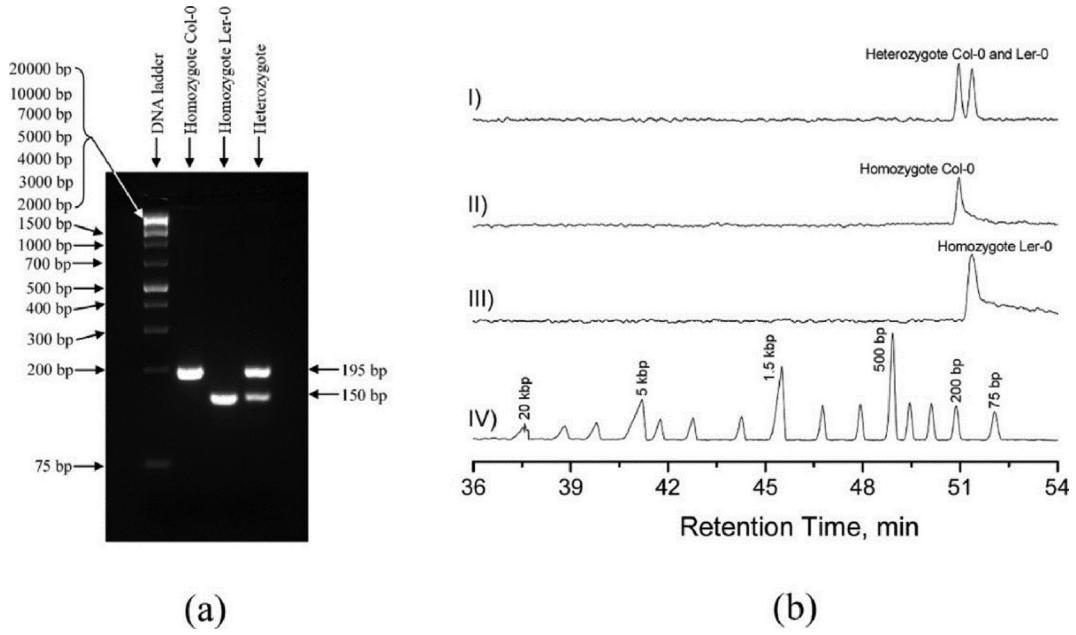

Figure 15. Separation results of *Arabidopsis* SSLP no. 38 PCR product. (a) Slab-gel separation result. (b) BaNC-HDC separation result. For BaNC-HDC separation: the separation capillary had a total length of 46 cm (42 cm effective). The eluent was 10 mM TE. The sample was injected at 100 psi for 5 s and the chamber pressure was 90 psi. Trace I, trace II, trace III and trace IV exhibit the results from a heterozygote sample, a homozygote of Col-0, a homozygote of Ler-0, and the GeneRuler 1-kb DNA ladder Plus, respectively. (Reprinted with permission from ref. 42. Copyright (2008) American Chemical Society).

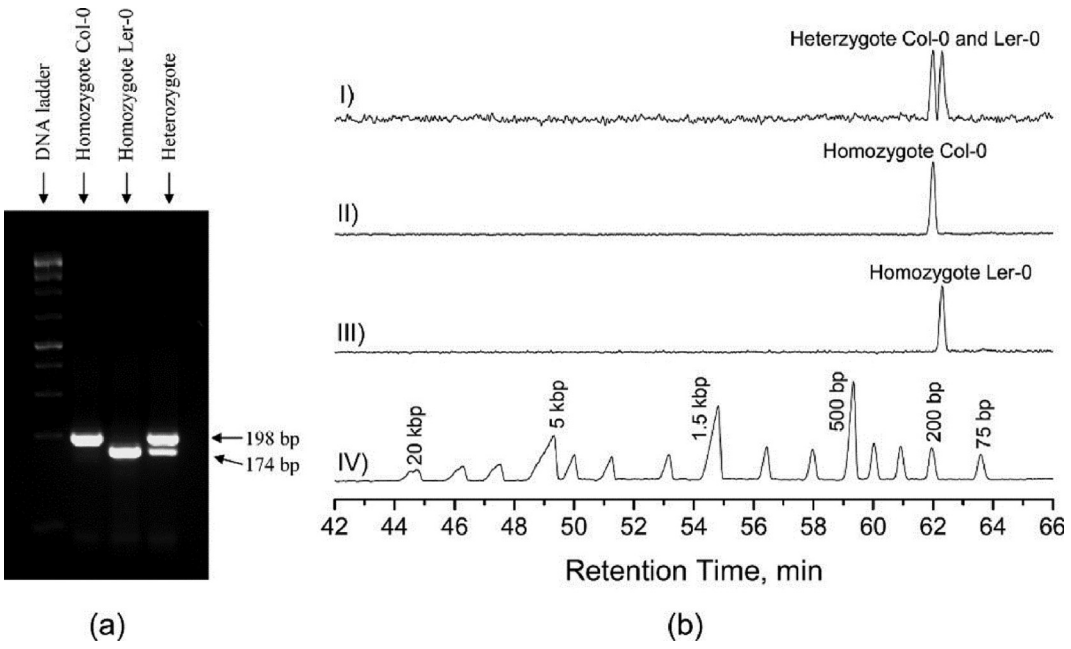

Figure 16. Separation results of *Arabidopsis* SSLP no. 47 PCR product. (a) Slab-gel separation result. (b) BaNC-HDC separation result. For BaNC-HDC separation: the separation capillary had a total length of 55 cm (51 cm effective). The sample was injected under 50 psi for 5 s and the chamber pressure was 110 psi. All other conditions were the same as described in Figure 14. (Reprinted with permission from ref. 42. Copyright (2008) American Chemical Society).

length as shown in Figure 13. However, as PFGE was difficult to realize the separation of both large and small DNA fragments in a single run, the smallest DNA fragment of 0.44 kbp was missing in the PFGE profile.

Zhu et al. [59] applied this approach to size plasmid DNA from *E-coli* and resolutions comparable to agarose gel electrophoresis were obtained. A linear DNA produced after the circular plasmid was digested by restriction enzyme *X*baI. Figure 14A shows the sizing results of plasmid DNA with BaNC-HDC. Using the relationship between the relative BaNC-HDC mobility and DNA fragment size based on the HDC quadratic model, the linear plasmid DNA fragment with a theoretical size value of 4.46 kbp was estimated to be 4.5 kbp. Because of the conformation of open circular and supercoiled DNA, multiple peaks were observed in the sample of plasmid DNA before digestion. Agarose gel electrophoresis was also used to analyze the same three samples, and comparable results were obtained. However, the separation time was shorted in BaNC-HDC and the sample required was less than that in agarose gel electrophoresis.

Zhu et al. [49] validated the feasibility of the method for DNA fragment quantitation in real-world sample. They used the calibration curves in Figure 5b to calculate the concentration and compute the number of molecules of the DNA fragments in digested λ-DNA sample with relative quantitation errors of around or less than 10%.

5.2. Genotyping analysis

This technique was also used to resolve real-world genotyping samples to demonstrate its practical applicability. Wang et al. [42] used nanocapillary HDC to analyze the *Arabidopsis* plant simple sequence length polymorphism (SSLP) sample. PCR-amplified DNA fragments without any further purifications were injected into the nanocapillary directly. Figure 15b presents the results of two genotyping analyses by BaNC-HDC. SSLP samples (no. 38) from heterozygote Col-0 and Ler-0 plants contained both a 195-bp fragment and a 150-bp fragment, while samples from homozygote Col-0 and samples from homozygote Ler-0 produced a 195 bp fragment and a 150-bp fragment, respectively. Figure 15a shows the results obtained by the slab-gel separation. Samples from heterozygous and homozygous individuals were both unambiguous identified using these two approaches. Furthermore, another SSLP samples (no. 47) in which the fragment difference was smaller than SSLP samples (no. 38) were also resolved with a slight increase in the capillary length and the elution pressure, and the results were displayed in Figure 16.

5.3. DNA conformation changes and DNA-biomolecule interaction analysis

Besides the analysis of length and quantification of DNA fragments, analysis of DNA conformation or conformational changes and interactions with other biomolecules are also the important research field for DNA analysis.

Friedrich et al. [62] utilized SML-FSHS to analyze the shape changes of DNA molecules in free solution. The average size of molecules was determined by HDC based on the peak retention time, and the molecules were observed under single molecule spectroscopy. So, the DNA conformations and distributions were determined by examining the size and the shape of each individual molecule. The conformation of stained double-strand DNA fragments was related to the shape of single molecule fluorescent bursts and the relative hydrodynamic mobility of the fragment. The authors [63] then applied the SML-FSHS platform to evaluate DNA-biomolecules interactions. Bound DNA-biomolecule complexes and unbound DNA molecule were separated by HDC and the size change resulted from binding was determined simultaneously. Quantitation of the DNA in the bound and unbound state which could characterize the binding behavior was performed using single molecule detection.

6. Conclusions

In conclusion, HDC is a powerful tool for DNA fragment sizing and quantitation in free solution. The method has the excellent feature that can separate both small and large DNA molecules at the same time compared to conventional gel electrophoresis and PFGE. The analysis uses only pL of sample, and its limit of detection has reached to the single-molecule level. With the incorporation of a micro-chip injector and EOP with BaNC-HDC, DNA fragments can be analyzed

with high speed, high resolution and high throughput. However, the technique currently still has several limitations. Due to the small diameter of the capillary column and pL-per-min flow rate, it is challenging to incorporate a mass spectrometer (MS) or a UV/Vis absorbance detector which will be helpful for fragment sequence analysis. Up to date, only LIF was used for HDC DNA analysis, and this will constrain the technique's application. The pL injection volume can also play adversely toward the spread of this method, because research often need to analyze samples with adequate volumes so that they can be representative to their original specimen. In other times, researchers may want to further analyze specific fragments after HDC separation. At the time being, it is difficult to collect the resolved fragments for these applications because of the low-micrometer- to nanometer-radius capillary column, pL-per-min flow rate and pL injection volume. Attentions are needed to filtrate the samples and eluents to prevent capillary clogging. With the technology advancement, we are confident that HDC will be incorporated with MS for DNA analysis. We also expect that HDC will be integrated on lab-on-a-chip devices for high-speed and high-throughput DNA analysis, and the platform can be an excellent tool for point-of-care analysis and patient-bedside clinical diagnose.

Declarations

Author contribution statement

All authors listed have significantly contributed to the development and the writing of this article.

Funding statement

This work was supported by the National Natural Science Foundation of China (NSFC Nos. 21625501, 21936001 and 21804005) and Beijing Outstanding Young Scientist Program (No. BJJWZYJH012019100 05017).

Data availability statement

Data will be made available on request.

Declartion of interests statement

The authors declare no conflict of interest.

Additional information

No additional information is available for this paper.

References

[1] K.O. Pedersen, Exclusion chromatography, Arch. Biochem. Biophys. Suppl 1 (1962) 157–168.
[2] E.A. DiMarzio, C.M. Guttman, Separation by flow, J. Polym. Sci., Part B 7 (4) (1969) 267–272.
[3] E.A. DiMarzio, C.M. Guttman, Separation by flow, Macromolecules 3 (2) (1970) 131–146.
[4] E.A. Dimarzio, C.M. Guttman, Separation by flow and its application to gel permeation chromatography, J. Chromatogr. 55 (1) (1971) 83–97.
[5] A.M. Striegel, Hamish small: experimenter extraordinaire. *Lc Gc N*, Am. For. 33 (10) (2015) 776–781.
[6] H. Small, Hydrodynamic chromatography. Technique for size analysis of colloidal particles, J. Colloid Interface Sci. 48 (1) (1974) 147–161.
[7] H. Small, M.A. Langhorst, Hydrodynamic chromatography, Anal. Chem. 54 (8) (1982) 892A–894A, 896A-898A.
[8] A.K. Brewer, A.M. Striegel, Particle size characterization by quadruple-detector hydrodynamic chromatography, Anal. Bioanal. Chem. 393 (1) (2009) 295–302.
[9] A.M. Striegel, S.L. Isenberg, G.L. Cote, An SEC/MALS study of alternan degradation during size-exclusion chromatographic analysis, Anal. Bioanal. Chem. 394 (7) (2009) 1887–1893.
[10] A.K. Brewer, A.M. Striegel, Characterizing string-of-pearls colloidal silica by multidetector hydrodynamic chromatography and comparison to multidetector size-exclusion chromatography, off-line multiangle static light scattering, and transmission electron microscopy, Anal. Chem. 83 (8) (2011) 3068–3075.
[11] A.K. Brewer, A.M. Striegel, Characterizing the size, shape, and compactness of a polydisperse prolate ellipsoidal particle via quadruple-detector hydrodynamic chromatography, Analyst 136 (3) (2011) 515–519.
[12] A.K. Brewer, A.M. Striegel, Characterizing a spheroidal nanocage drug delivery vesicle using multi-detector hydrodynamic chromatography, Anal. Bioanal. Chem. 399 (4) (2011) 1507–1514.
[13] A.M. Striegel, Hydrodynamic chromatography: packed columns, multiple detectors, and microcapillaries, Anal. Bioanal. Chem. 402 (1) (2012) 77–81.
[14] F.W. Studier, Slab-gel electrophoresis, Trends Biochem. Sci. 25 (12) (2000) 588–590.
[15] E.S. Nassonova, Pulsed field gel electrophoresis: theory, instruments and application, Cell Tissue Biol. 2 (6) (2008) 557–565.
[16] H.J. Jung, Y.C. Bae, Theory for the capillary electrophoretic separation of DNA in polymer solutions, J. Chromatogr. A 967 (2) (2002) 279–287.
[17] B.C. Durney, C.L. Crihfield, L.A. Holland, Capillary electrophoresis applied to DNA: determining and harnessing sequence and structure to advance bioanalyses (2009–2014), Anal. Bioanal. Chem. 407 (23) (2015) 6923–6938.
[18] N.A. Olson, J. Khandurina, A. Guttman, DNA profiling by capillary array electrophoresis with non-covalent fluorescent labeling, J. Chromatogr. A 1051 (1) (2004) 155–160.
[19] B.M. Olivera, P. Baine, N. Davidson, Electrophoresis of the nucleic acids, Biopolymers 2 (3) (1964) 245–257.
[20] J. Noolandi, A new concept for sequencing DNA by capillary electrophoresis, Electrophoresis 13 (1) (1992) 394–395.
[21] P. Mayer, G.W. Slater, G. Drouin, Theory of DNA sequencing using free-solution electrophoresis of protein-DNA complexes, Anal. Chem. 66 (10) (1994) 1777–1780.
[22] C. Heller, G.W. Slater, P. Mayer, N. Dovichi, D. Pinto, J.-L. Viovy, G. Drouin, Free-solution electrophoresis of DNA, J. Chromatogr. A 806 (1) (1998) 113–121.
[23] X. Liu, M.M. Skanata, D. Stein, Entropic cages for trapping DNA near a nanopore, Nat. Commun. 6 (2015) 6222.
[24] E.S. Rodriguez, S.C. Lam, P.R. Haddad, B. Paull, Reversed-phase functionalised multi-lumen capillary as combined concentrator, separation column, and ESI emitter in capillary-LC-MS, Chromatographia 82 (1) (2019) 197–209.
[25] L.R. Huang, J.O. Tegenfeldt, J.C. Sturm, R.H. Austin, E.C. Cox, A DNA prism: physical principles for optimizing a microfabricated DNA separation device, Tech. Digest Int. Elect. Devices Meet. (2002) 211–214.
[26] L.R. Huang, J.O. Tegenfeldt, J.J. Kraeft, J.C. Sturm, R.H. Austin, E.C. Cox, A DNA prism for high-speed continuous fractionation of large DNA molecules, Nat. Biotechnol. 20 (10) (2002) 1048–1051.
[27] A. Sabarudin, J. Huang, S. Shu, S. Sakagawa, T. Umemura, Preparation of methacrylate-based anion-exchange monolithic microbore column for chromatographic separation of DNA fragments and oligonucleotides, Anal. Chim. Acta 736 (2012) 108–114.
[28] L. Zhang, B. Majeed, L. Lagae, P. Peumans, C. Van Hoof, W. De Malsche, Ion-pair reversed-phase chromatography of short double-stranded deoxyribonucleic acid in silicon micro-pillar array columns: retention model and applications, J. Chromatogr. A 1294 (2013) 1–9.
[29] C. Liang, J.-Q. Qiao, H.-Z. Lian, A novel strategy for retention prediction of nucleic acids with their sequence information in ion-pair reversed phase liquid chromatography, Talanta 185 (2018) 592–601.
[30] A. Shimoyama, A. Fujisaka, S. Obika, Evaluation of size-exclusion chromatography for the analysis of phosphorothioate oligonucleotides, J. Pharmaceut. Biomed. Anal. 136 (2017) 55–65.
[31] H. Ellegren, T. Laas, Size-exclusion chromatography of DNA restriction fragments. Fragment length determinations and a comparison with the behavior of proteins in size-exclusion chromatography, J. Chromatogr. 467 (1) (1989) 217–226.
[32] J.M. Schmitter, Y. Mechulam, G. Fayat, M. Anselme, Rapid purification of DNA fragments by high-performance size-exclusion chromatography, J. Chromatogr. Biomed. Appl. 378 (2) (1986) 462–466.
[33] J. Hirabayashi, N. Ito, K. Noguchi, K. Kasai, Slalom chromatography: size-dependent separation of DNA molecules by a hydrodynamic phenomenon, Biochemistry 29 (41) (1990) 9515–9521.
[34] Y.C. Guillaume, E. Peyrin, M. Thomassin, A. Ravel, C. Grosset, A. Villet, J.-F. Robert, C. Guinchard, Column efficiency and separation of DNA fragments using slalom chromatography: hydrodynamic study and fractal considerations, Anal. Chem. 72 (20) (2000) 4846–4852.
[35] E. Peyrin, Y.C. Guillaume, A. Villet, A. Ravel, C. Grosset, J. Alary, A. Favier, Flow rate dependence on the biopolymer retention in hydrodynamic chromatography. Comparison between the behaviors of proteins and plasmids, J. Liq. Chromatogr. Relat. Technol. 24 (9) (2001) 1245–1252.
[36] Y. Liu, W. Radke, H. Pasch, Coil-stretch transition of high molar mass polymers in packed-column hydrodynamic chromatography, Macromolecules 38 (17) (2005) 7476–7484.
[37] X.Y. Wang, L. Liu, W. Wang, Q.S. Pu, G.S. Guo, P.K. Dasgupta, S.R. Liu, Resolving DNA in free solution, Trends Anal. Chem. 35 (2012) 122–134.
[38] W. Zhang, L. Liu, Q. Zhang, D. Zhang, Q. Hu, Y. Wang, X. Wang, Q. Pu, G. Guo, Visual and real-time imaging focusing for highly sensitive laser-induced fluorescence detection at yoctomole levels in nanocapillaries, Chem. Commun. 56 (2020) 2423–2426.
[39] P. Xiang, Y. Zhu, Y. Yang, Z. Zhao, S.M. Williams, R.J. Moore, R.T. Kelly, R.D. Smith, S. Liu, Picoflow liquid chromatography-mass spectrometry for

ultrasensitive bottom-up proteomics using 2-μm-i.d. Open tubular columns, Anal. Chem. 92 (7) (2020) 4711–4715.
[40] P. Xiang, Y. Yang, Z. Zhao, J. Wang, M. Chen, A. Chen, S. Liu, Performing flow injection chromatography using a narrow open tubular column, Anal. Chim. Acta 1109 (2020) 19–26.
[41] X.Y. Wang, J.Z. Kang, S.L. Wang, J.J. Lu, S.R. Liu, Chromatographic separations in a nanocapillary under pressure-driven conditions, J. Chromatogr. A 1200 (2) (2008) 108–113.
[42] X.Y. Wang, S.L. Wang, V. Veerappan, C.K. Byun, H. Nguyen, B. Gendhar, R.D. Allen, S.R. Liu, Bare nanocapillary for DNA separation and genotyping analysis in gel-free solutions without application of external electric field, Anal. Chem. 80 (14) (2008) 5583–5589.
[43] A.M. Striegel, A.K. Brewer, Hydrodynamic chromatography, Annu. Rev. Anal. Chem. 5 (2012) 15–34.
[44] H. Brenner, L.J. Gaydos, The constrained brownian movement of spherical particles in cylindrical pores of comparable radius: models of the diffusive and convective transport of solute molecules in membranes and porous media, J. Colloid Interface Sci. 58 (2) (1977) 312–356.
[45] R. Tijssen, J. Bos, M.E. Van Kreveld, Hydrodynamic chromatography of macromolecules in open microcapillary tubes, Anal. Chem. 58 (14) (1986) 3036–3044.
[46] X.Y. Wang, L. Liu, Q.S. Pu, Z.F. Zhu, G.S. Guo, H. Zhong, S.R. Liu, Pressure-induced transport of DNA confined in narrow capillary channels, J. Am. Chem. Soc. 134 (17) (2012) 7400–7405.
[47] J.H. Knox, M.T. Gilbert, Kinetic optimization of straight open-tubular liquid chromatography, J. Chromatogr. A 186 (1979) 405–418.
[48] D. Stein, F.H. van der Heyden, W.J. Koopmans, C. Dekker, Pressure-driven transport of confined DNA polymers in fluidic channels, Proc. Natl. Acad. Sci. U.S.A. 103 (43) (2006) 15853–15858.
[49] Z. Zhu, H. Chen, A. Chen, J.J. Lu, S. Liu, M. Zhao, Simultaneously sizing and quantitating zeptomole-level DNA at high throughput in free solution, Chem. Eur J. 20 (43) (2014) 13945–13950.
[50] Z.F. Zhu, L. Liu, W. Wang, J.J. Lu, X.Y. Wang, S.R. Liu, Resolving DNA at efficiencies of more than a million plates per meter using bare narrow open capillaries without sieving matrices, Chem. Commun. 49 (28) (2013) 2897–2899.
[51] X.Y. Wang, V. Veerappan, C. Cheng, X. Jiang, R.D. Allen, P.K. Dasgupta, S.R. Liu, Free solution hydrodynamic separation of DNA fragments from 75 to 106 000 base pairs in A single run, J. Am. Chem. Soc. 132 (1) (2010) 40–41.
[52] L. Liu, V. Veerappan, Q.S. Pu, C. Cheng, X.Y. Wang, L.P. Lu, R.D. Allen, G.S. Guo, High-resolution hydrodynamic chromatographic separation of large DNA using narrow, bare open capillaries: a rapid and economical alternative technology to pulsed-field gel electrophoresis? Anal. Chem. 86 (1) (2014) 729–736.
[53] K.J. Liu, T.D. Rane, Y. Zhang, T.H. Wang, Single-molecule analysis enables free solution hydrodynamic separation using yoctomole levels of DNA, J. Am. Chem. Soc. 133 (18) (2011) 6898–6901.
[54] K.J. Liu, T.H. Wang, Cylindrical illumination confocal spectroscopy: rectifying the limitations of confocal single molecule spectroscopy through one-dimensional beam shaping, Biophys. J. 95 (6) (2008) 2964–2975.
[55] C.W. Beh, D. Pan, J. Lee, X. Jiang, K.J. Liu, H.Q. Mao, T.H. Wang, Direct interrogation of DNA content distribution in nanoparticles by a novel microfluidics-based single-particle analysis, Nano Lett. 14 (8) (2014) 4729–4735.
[56] R.N. Li, L. Liu, Y. Wang, X.Y. Wang, Effect of temperature on DNA chromatographic separation in free solution, Chem. Lett. 41 (11) (2012) 1506–1508.
[57] L. Liu, V. Veerappan, Y.Z. Bian, G.S. Guo, X.Y. Wang, Influence of elution conditions on DNA transport behavior in free solution by hydrodynamic chromatography, Sci. China Chem. 58 (10) (2015) 1605–1611.
[58] M.T. Weaver, K.B. Lynch, Z.F. Zhu, H. Chen, J.J. Lu, Q.S. Pu, S.R. Liu, Confocal laser-induced fluorescence detector for narrow capillary system with yoctomole limit of detection, Talanta 165 (2017) 240–244.
[59] Z.F. Zhu, H. Chen, W. Wang, A. Morgan, C.Y. Gu, C.Y. He, J.J. Lu, S.R. Liu, Integrated bare narrow Capillary Hydrodynamic chromatographic system for free-solution DNA separation at the single-molecule level, Angew. Chem. Int. Ed. 52 (21) (2013) 5612–5616.
[60] C. He, J.J. Lu, Z. Jia, W. Wang, X. Wang, P.K. Dasgupta, S. Liu, Flow batteries for microfluidic networks: configuring an electroosmotic pump for nonterminal positions, Anal. Chem. 83 (7) (2011) 2430–2433.
[61] H. Chen, Z.F. Zhu, J.J. Lu, S.R. Liu, Charging YOYO-1 on capillary wall for online DNA intercalation and integrating this approach with multiplex PCR and bare narrow capillary-hydrodynamic chromatography for online DNA analysis, Anal. Chem. 87 (3) (2015) 1518–1522.
[62] S.M. Friedrich, K.J. Liu, T.H. Wang, Single molecule hydrodynamic separation allows sensitive and quantitative analysis of DNA conformation and binding interactions in free solution, J. Am. Chem. Soc. 138 (1) (2016) 319–327.
[63] S.M. Friedrich, R. Bang, A. Li, T.H. Wang, Versatile analysis of DNA-biomolecule interactions in solution by hydrodynamic separation and single molecule detection, Anal. Chem. 91 (4) (2019) 2822–2830.